Journal of Coastal Research	15	3	766–773	Royal Palm Beach, Florida	Summer 1999

Bottom Stress of Wind-Driven Currents Over an Inner Shelf Determined from Depth-Integrated Storm Surge Model

Sung-Chan Kim† and Jye Chen‡

†College of William and Mary
School of Marine Science
Gloucester Point, VA 23062,
USA

‡Techniques Development
Laboratory
NWS/NOAA
Silver Spring, MD 20910,
USA

ABSTRACT

KIM, S. and CHEN, J., 1999. Bottom Stress of Wind-Driven Currents Over an Inner Shelf Determined from Depth-Integrated Storm Surge Model. *Journal of Coastal Research,* 15(3), 766–773. Royal Palm Beach (Florida), ISSN 0749-0208.

Bottom stress from wind-driven current was explicitly calculated using the SLOSH (Sea, Lake, and Overland Surges from Hurricanes) model in which the bottom stress is not collinear with the direction of depth-averaged flow. The asymptotic behavior of wind-flow relationships in a shallow ocean with a horizontally infinite extent shows that the SLOSH model estimates reasonably the magnitude and the direction of the bottom stress over a range of the shallow water condition. For the broad and shallow inner shelf of the Middle Atlantic Bight (MAB), the SLOSH model for steady flow for a semi-infinite ocean resulted in reasonable estimation of bottom flow under the high wind conditions of typical extratropical origin.

ADDITIONAL INDEX WORDS: *Bottom stress, wind-driven current, inner shelf, coastal circulation, storm surges.*

INTRODUCTION

In the intermediate water depths over an inner shelf, comparable to the Ekman layer thickness, the flow behavior contains both rotational deep-water boundary layer and collinear shallow water boundary layer flow structures. Detached surface and bottom boundary layers over an outer and mid shelf become merging over an inner shelf. LENTZ (1995) gave a dynamic definition of an inner shelf as a transition region characterized by a cross-shelf divergence in the Ekman transport due to the interaction of the surface and the bottom boundary layers. He also demonstrated that the inner-shelf circulation is sensitive to the eddy viscosity profile. In the bottom boundary layer, the eddy viscosity is related to bottom friction velocity, u_{*_b}, which in turn is a function of the bottom stress ($\mathrm{Amp}(\tau_b) = \rho u_{*_b}^2$ where ρ is water density). The bottom stress of the wind-driven currents is known to determine the diffusion and the flux gradient of suspended sediment concentration and thus has a critical role in coastal morphodynamics (*e.g.,* WRIGHT, 1995).

The SLOSH (Sea, Lake, and Overland Surges from Hurricane) model was developed for real-time forecast of coastal storm surges (JELESNIANSKI *et al.,* 1992) and has been being maintained as an operational model by the US National Weather Services (NWS). The SLOSH model has been also successfully applied for extratropical storm surges (*e.g.,* KIM *et al.,* 1996; BLIER *et al.,* 1997; KIM *et al.,* 1998) by replacing its unique parametric storm structure with synoptic scale winds from variable global atmospheric models such as the Avn and the ECMWF models. The SLOSH model is not simply a vertically averaged two-dimensional model but instead it is based on a flow structure assumption. The flow structure is primarily controlled by bottom stress which is not collinear with depth-averaged velocity (JELESNIANSKI, 1970). JENTER and MADSEN (1989), (JM hereafter), examined the bottom stress of wind-driven flows in a coastal sea using a depth-resolving model (JM model hereafter). They demonstrated that the conventional drag formulation would be unlikely to predict correctly the bottom stress direction given depth-averaged velocity. In the same context, DAVIES (1988) pointed out that, for wind driven flows, the bed stress determined from a vertically integrated two-dimensional model was significantly different from that computed using a fully three-dimensional model.

The objective of this study is to investigate the SLOSH model bottom stress formulation by comparing it with the JM model for steady wind-driven currents in coastal waters. We will explore the usability of the SLOSH model bottom formulation for near-bottom flow characteristics, while acknowledging the inherent weakness of using constant eddy viscosity. First, an ocean of infinite horizontal extent was used to study the asymptotic behavior of the nearshore steady wind-driven flow. Then we applied both models for the semi-infinite ocean—simplification of the Middle Atlantic Bight (MAB) off the North Carolina coast. Transports and bottom stresses were simulated during the one-month period of October 1994. The observation data from the bottom boundary

98120 received 13 April 1998; accepted in revision 17 August 1998.

measurement tripod of the Virginia Institute of Marine Science (VIMS) during the same period was compared with model simulations.

THE SLOSH MODEL BOTTOM STRESS FORMULATION

We use the vertical coordinate, z, and the horizontal coordinate, $Z = x+iy$, such that u and v are velocities in the x- and y-directions of Cartesian coordinate, respectively. For a linear, homogeneous water column, the complex notation of momentum equation (*e.g.* WELANDER, 1961) becomes

$$\frac{\partial w}{\partial t} + ifw = q + \frac{\partial}{\partial z}\left(\nu\frac{\partial w}{\partial z}\right) \tag{1}$$

where horizontal velocity is

$$w = u + iv \tag{2}$$

and horizontal pressure gradient is

$$q = -g\left(\frac{\partial \eta}{\partial x} + i\frac{\partial \eta}{\partial y}\right). \tag{3}$$

Here, $i(=\sqrt{-1})$ denotes the complex number; η is water level; g is gravitational acceleration; f is Coriolis parameter; and ν is eddy viscosity. If we integrate equation (1) over water depth, we have

$$\frac{\partial W}{\partial t} + ifW = Q + R - T \tag{4}$$

where we define transport as the depth integrated horizontal velocity

$$W = \int_{z_0}^{h} w\, dz = U + iV. \tag{5}$$

Surface stress term is defined as

$$R = \frac{\tau_s}{\rho} \tag{6}$$

bottom stress term is

$$T = \frac{\tau_b}{\rho} \tag{7}$$

and gradient term is

$$Q = qh \tag{8}$$

Here, τ_s is surface stress, τ_b is bottom stress, and ρ is water density. The solution of equation (4) depends on bottom stress term, T, which is difficult to obtain from the depth integrated transport. PLATZMAN (1963) assumed constant eddy viscosity (ν = 0.0225 m²/sec) and introduced a time operator

$$\sigma^2 = \frac{h^2}{\nu}\left(if + \frac{\partial}{\partial t}\right) = \sigma_0^2 + \lambda \tag{9}$$

so that

$$\sigma_0^2 = if\frac{h^2}{\nu} \tag{10}$$

and

$$\lambda = \frac{h^2}{\nu}\frac{\partial}{\partial t}. \tag{11}$$

JELESNIANSIK *et al.* (1992) introduced a slip boundary condition at the bed (z = 0) with slip coefficient (s = 0.0009 m/sec) so that $T = sw|_{z=0}$. They eliminated the bottom stress term by using a convolution method. Thereby, the transport equation becomes

$$\frac{\partial W}{\partial t} + ifAW = BQ + CR \tag{12}$$

Here, complex coefficients are given by

$$A = \frac{1 + \dfrac{G_0}{\sigma_0^2}}{1 + G_1} \tag{13}$$

$$B = \frac{1}{1 + G_1} \tag{14}$$

and

$$C = \frac{1 + H_0}{1 + G_1} \tag{15}$$

where

$$\frac{G_0}{\sigma_0^2} = \frac{1}{\sigma_0 \coth \sigma_0 + if\dfrac{h}{s} - 1} \tag{16}$$

$$G_1 = \left(\frac{G_0}{\sigma_0^2}\right)^2\left[\frac{1}{2}(\sigma_0 \coth \sigma_0 + \sigma_0^2 \operatorname{csch}^2\sigma_0) - 1\right] \tag{17}$$

and

$$H_0 = \frac{1 - \sigma_0 \operatorname{csch} \sigma_0}{\sigma_0 \coth \sigma_0 + if\dfrac{h}{s} - 1}. \tag{18}$$

One should note that all the coefficients become functions of the water depth, the eddy viscosity, the Coriolis parameter, and the slip coefficient. The choice of the values for ν and s are based on the calibration for the high wind. The complex coefficients, A, B, and C, effectively include the bottom stress term. From equations (4) and (12), we can calculate the bottom stress term given transport, pressure gradient, and surface wind stress

$$T = -if(1 - A)W + (1 - B)Q + (1 - C)R \tag{19}$$

For steady current, equation (12) gives transport

$$W = \frac{BQ + CR}{ifA} \tag{20}$$

Then, the bottom stress term in equation (19) becomes

$$T = (1 - B/A)Q + (1 - C/A)R \tag{21}$$

THE JM MODEL BOTTOM STRESS FORMULATION

The JM model is based on a more realistic bilinear eddy viscosity

$$\nu = \begin{cases} \kappa u_{*s}(h - z) & \text{for } z > z_m \\ \kappa u_{*b} z & \text{for } z < z_m \end{cases} \tag{22}$$

where κ is the Von Karman constant and $u_{*s} = \sqrt{[\mathrm{Amp}(\tau_s)]/\rho}$ is surface friction velocity and $u_{*b} = \sqrt{[\mathrm{Amp}(\tau_b)]/\rho}$ is bottom friction velocity. The mid-depth where the eddy viscosity is continuous is defined as

$$z_m = h\frac{u_{*b}}{u_{*s} + u_{*b}}. \tag{23}$$

Equation (1) is rearranged for steady state

$$\frac{d}{dz}\left(\nu\frac{dw^*}{dz}\right) - ifw^* = 0 \tag{24}$$

where

$$w^* = w + i\frac{q}{f}. \tag{25}$$

Introducing new length scales

$$z_b = \frac{z}{\kappa u_{*b}/f} \quad \text{and} \quad \zeta_b = 2\sqrt{z_b}$$

$$z_s = \frac{h - z}{\kappa u_{*s}/f} \quad \text{and} \quad \zeta_s = 2\sqrt{z_s}. \tag{26}$$

Then the solution becomes

$$w_b^* = A_b(\mathrm{ber}\zeta_b + i\mathrm{bei}\zeta_b) + B_b(\mathrm{ker}\zeta_b + i\mathrm{kei}\zeta_b) \quad \text{for } \zeta_b < \zeta_{bm} \tag{27}$$

$$w_s^* = A_s(\mathrm{ber}\zeta_s + i\mathrm{bei}\zeta_s) + B_s(\mathrm{ker}\zeta_s + i\mathrm{kei}\zeta_s) \quad \text{for } \zeta_s > \zeta_{sm}. \tag{28}$$

Here, A_b, B_b, A_s, and B_s are the complex constants to be determined from boundary conditions.

At the bottom, no slip boundary condition is applied

$$w_b^*|_{\zeta_b=\zeta_{b0}} = i\frac{q}{f}. \tag{29}$$

At the surface, wind stress is applied

$$\frac{\tau_s}{\rho} = u_{*s}^2 e^{i\phi} = -\kappa u_{*s}\frac{\zeta_s}{2}\left.\frac{dw_s^*}{d\zeta_s}\right|_{\zeta_s\to 0} \tag{30}$$

where ϕ is the wind direction. At mid depth, velocities and shears from surface and bottom layers are equated

$$w_b^*|_{\zeta_b=\zeta_{bm}} = w_s^*|_{\zeta_s=\zeta_{sm}} \tag{31}$$

$$\kappa u_{*b}\frac{\zeta_{bm}}{2}\left.\frac{dw_b^*}{d\zeta_b}\right|_{\zeta_b=\zeta_{bm}} = -\kappa u_{*s}\frac{\zeta_{sm}}{2}\left.\frac{dw_s^*}{d\zeta_s}\right|_{\zeta_s=\zeta_{sm}}. \tag{32}$$

From equations (27) through (30), we have a set of simultaneous equations

$$\Delta\cdot\mathrm{X} = \mathrm{Y} \tag{33}$$

where

$$\Delta = \begin{bmatrix} \mathrm{ber}\zeta_{b0} + i\mathrm{bei}\zeta_{b0} & \mathrm{ker}\zeta_{b0} + i\mathrm{kei}\zeta_{b0} \\ 0 & 0 \\ \mathrm{ber}\zeta_{bm} + i\mathrm{bei}\zeta_{bm} & \mathrm{ker}\zeta_{bm} + i\mathrm{kei}\zeta_{bm} \\ \mathrm{ber}'\zeta_{bm} + i\mathrm{bei}'\zeta_{bm} & \mathrm{ker}'\zeta_{bm} + i\mathrm{kei}'\zeta_{bm} \end{bmatrix}$$

$$\begin{bmatrix} 0 & 0 \\ \mathrm{ber}'\zeta_{s0} + i\mathrm{bei}'\zeta_{s0} & \mathrm{ker}'\zeta_{s0} + i\mathrm{kei}'\zeta_{s0} \\ -(\mathrm{ber}\zeta_{sm} + i\mathrm{bei}\zeta_{sm}) & -(\mathrm{ker}\zeta_{sm} + i\mathrm{kei}\zeta_{sm}) \\ \gamma(\mathrm{ber}'\zeta_{sm} + i\mathrm{bei}'\zeta_{sm}) & \gamma(\mathrm{ker}'\zeta_{sm} + i\mathrm{kei}'\zeta_{sm}) \end{bmatrix} \tag{34}$$

$$\mathrm{X} = \begin{bmatrix} A_b \\ B_b \\ A_s \\ B_s \end{bmatrix} \tag{35}$$

$$\mathrm{Y} = \begin{bmatrix} i\frac{q}{f} \\ -\frac{2u_{*s}}{\kappa\zeta_{s0}}e^{i\phi} \\ 0 \\ 0 \end{bmatrix} \tag{36}$$

and

$$\gamma = \frac{u_{*s}}{u_{*b}}\frac{\zeta_{sm}}{\zeta_{bm}}. \tag{37}$$

The solution requires an iteration for u_{*b}. The bottom stress term becomes

$$T = \frac{\kappa u_{*b}\zeta_{b0}}{2}(A_b(\mathrm{ber}'\zeta_{b0} + i\mathrm{bei}'\zeta_{b0}) + B_b(\mathrm{ker}'\zeta_{b0} + i\mathrm{kei}'\zeta_{b0})). \tag{38}$$

The transport becomes

$$\begin{aligned} W = \frac{i}{f}\Bigg[&\frac{\kappa u_{*s}}{2}\{\zeta_{s0}A_s(\mathrm{ber}'\zeta_{s0} + i\mathrm{ber}'\zeta_{s0}) + \zeta_{s0}B_s(\mathrm{ker}'\zeta_{s0} + i\mathrm{ker}'\zeta_{s0}) \\ &- \zeta_{sm}A_s(\mathrm{ber}'\zeta_{sm} + i\mathrm{ber}'\zeta_{sm}) \\ &+ \zeta_{sm}B_s(\mathrm{ker}'\zeta_{sm} + i\mathrm{ker}'\zeta_{sm})\} \\ &+ \frac{\kappa u_{*b}}{2}\{\zeta_{b0}A_b(\mathrm{ber}'\zeta_{b0} + i\mathrm{ber}'\zeta_{b0}) \\ &+ \zeta_{b0}B_b(\mathrm{ker}'\zeta_{b0} + i\mathrm{ker}'\zeta_{b0}) \\ &- \zeta_{bm}A_b(\mathrm{ber}'\zeta_{bm} + i\mathrm{ber}'\zeta_{bm}) \\ &+ \zeta_{bm}B_b(\mathrm{ker}'\zeta_{bm} + i\mathrm{ker}'\zeta_{bm})\} - Q\Bigg]. \end{aligned} \tag{39}$$

The steady solution depends on two length scales—bottom

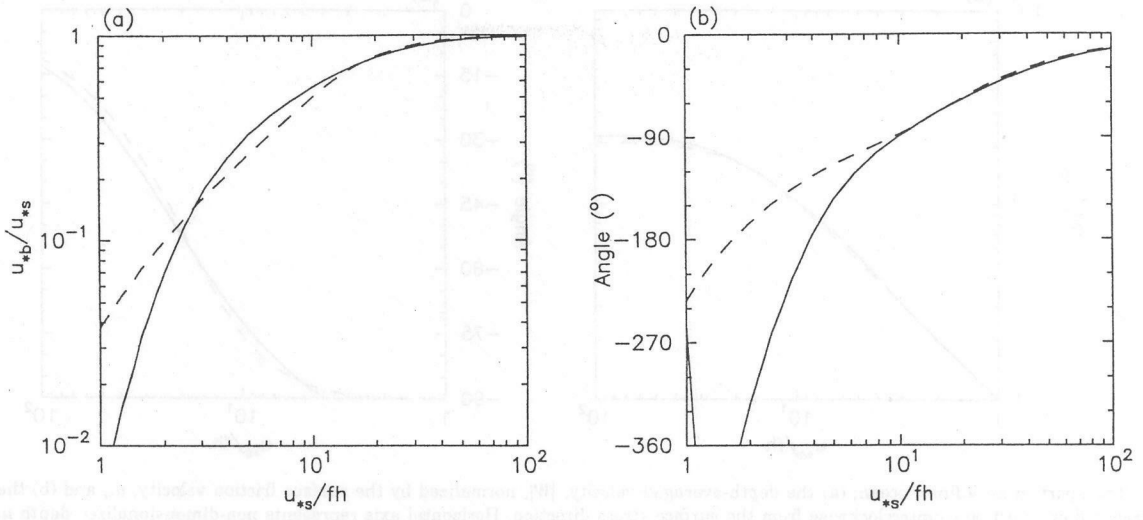

Figure 1. Bottom stress in an infinite ocean; (a) the bottom friction velocity, u_{*b}, normalized by the surface friction velocity, u_{*s} and (b) the angle of bottom stress direction counterclockwise from the surface stress direction. Horizontal axis represents non-dimensionalized depth u_{*s}/fh in which the lower value represents deep water and weak wind and the higher value denotes shallow water and strong wind. Solid line represents the SLOSH model while the dashed line represents the JM model.

roughness, z_{b0}, and a small length from the sea surface, z_{s0}. JM tabulated the range of the bottom roughness length scale based on the bottom sediment type. GRANT and MADSEN (1986) stated that z_{b0} is controlled by the distributed roughness, the wave-current interaction, the movable bed effect, and the suspended sediment concentration induced stratification. LENTZ (1995) showed no sensitivity of z_{s0} in two-dimensional eddy viscosity model. We took $z_{s0} = z_{b0}$ for simplicity in this study. The solution of the JM model involves an iteration procedure to converge to a value of bottom friction velocity, u_{*b}.

ASYMPTOTIC BEHAVIOR OF A HORIZONTALLY INFINITE OCEAN

JM took the ocean of infinite horizontal extent without geostrophic current to show the stress-velocity relationship. They demonstrated that the bottom stress and depth-averaged flow are never aligned. They also showed the dependency on bottom roughness. The SLOSH model was tested for the same setting in which $q = 0$. We assumed $z_{0b}/h = 10^{-6}$ which is for sandy bottom in the depth range of 10 to 100 m. We also assumed u_{*s}=1 cm/s. Using WU's (1982) formula for drag coefficient for surface winds, the wind speed of 10 m/s at 10 m above the mean sea level results in u_{*s}~1.2 cm/s. We investigated the results over a non-dimensionalized depth, u_{*s}/fh, which is the ratio of the surface Ekman layer depth to the water depth.

Figure 1 shows the bottom stress response to the surface stress. At the shallow depth (high u_{*s}/fh), the bottom stress approaches the surface stresses both in magnitude and direction. As the water depth increases (lower u_{*s}/fh), the bottom stress magnitude decreases and its direction veers to the right of that of the surface stress. The SLOSH model and the JM model agree well for high values of u_{*s}/fh. For shallow water, the bottom friction becomes identical to the surface friction (for $u_{*s}/fh \gg 10$, $u_{*b} \sim u_{*s}$). For deep water, no bottom friction effect from surface winds (for $u_{*s}/fh \ll 10$, $u_{*b} < 0.1\ u_{*s}$). The magnitude and direction of the bottom stress from both models deviate for $u_{*s}/fh < 10$ which corresponds to $h >$ 100 m. This lower limit is not considered relevant because resulting sediment transport in such deep water or from such weak surface winds would be negligible.

The transport (Figure 2) shows better agreement between two models in both magnitude and direction over all the ranges of u_{*s}/fh. The linear relationships between $|W|/u_{*s}$ and u_{*s}/fh are maintained for $u_{*s}/fh < 10$. JM explained that the large u_{*s}/fh limit is the turbulent Couette flow limit ($u_{*s} = u_{*b}$) where a constant stress profile is approached. Both models clearly show the shallow water limits (high u_{*s}/fh) of the collinear transport with the surface stress and the deep water limits (low u_{*s}/fh) of the typical Ekman transport in the right angle to the surface stress. The seemingly good agreement between the SLOSH and the JM models in this test should be interpreted with caution. JM showed that for $u_{*s}/fh > 10$ the dependence of transport on bottom roughness increases. Decreasing bottom roughness increases $|W|/u_{*s}$ as well as the veering angle. The higher value of $|W|/u_{*s}$ from the SLOSH model suggests that both models would have better agreement for the lower roughness length than $z_{0b}/h = 10^{-6}$.

SIMULATION FOR A SEMI-INFINITE OCEAN

The meteorological response of the morphodynamics over the MAB inner shelf off North Carolina during October 1994 was described by KIM *et al.* (1997). To test both models, the simulation included the same period of the VIMS bottom boundary measurement tripod deployment. The study area has a simple long coastline and a broad shelf where the isobaths are nearly parallel to the coastline (Figure 3). The

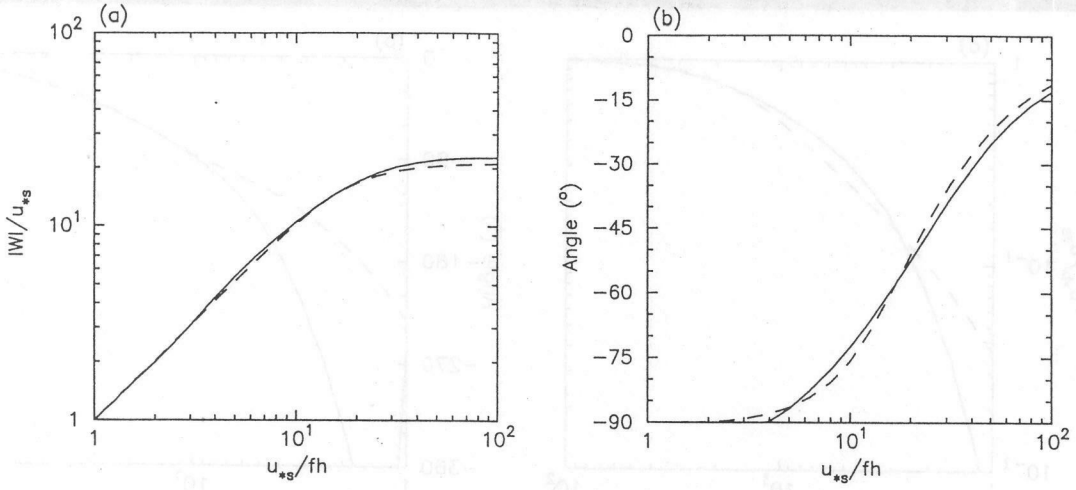

Figure 2. Transport in an infinite ocean; (a) the depth-averaged velocity, $|W|$, normalized by the surface friction velocity, u_{*_s} and (b) the angle of the depth-averaged flow direction counterclockwise from the surface stress direction. Horizontal axis represents non-dimensionalized depth u_*/fh in which the lower value represents deep water and weak wind and the higher value denotes shallow water and strong wind. Solid line represents the SLOSH model while the dashed line represents the JM model.

steady flow assumption is reasonable with the large-scale extratropical meteorological conditions prevailing over the MAB between fall and spring. We set the positive x-axis as the offshore direction. The positive y-axis is aligned with a coastline which is 20° counterclockwise from true north. We assumed a semi-infinite ocean of 20 m depth in which both the cross-shore transport term and the alongshore pressure gradient term approach zero. The net zero cross-shelf transport assumption has been accepted by many and is less questionable (*e.g.*, LENTZ, 1994). The second assumption of $\partial\eta/\partial y \rightarrow 0$ is not really supported by measurements (*e.g.*, LENTZ and WINANT, 1986). Steady solution requires iteration for both models. We first assumed a value for the cross-shore pressure gradient. The models then calculated W and T. With updated Q, the model calculations were repeated. The convergence criteria was given by $U \rightarrow 0$.

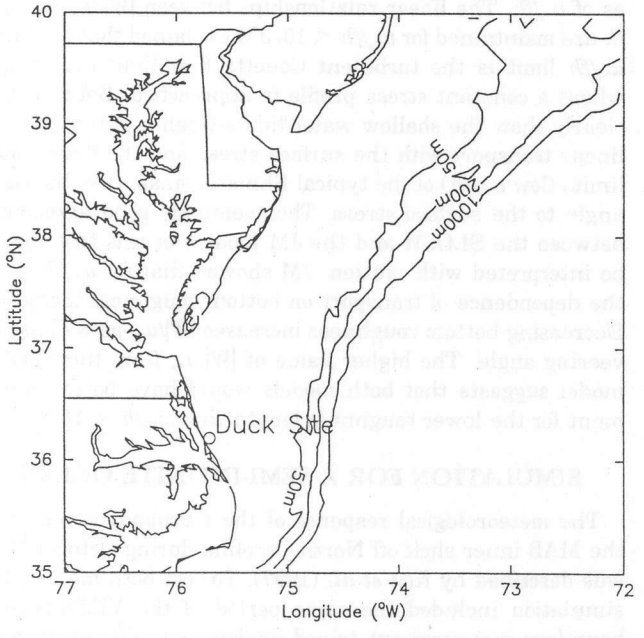

Figure 3. Location map for Duck site and the Middle Atlantic Bight.

We took one month anemometer data at 19.5-m above the mean sea level from the US Army Corp of Engineers Field Research Facility (FRF) at Duck, North Carolina (Figure 4). LENTZ (1994) showed that the observed wind near the coast may be lower than the surface wind in the deep water because of large gradients in wind stress magnitude near the coast. Thus we adopted WU's (1982) surface drag coefficient at 10-m above sea surface ($C_{10} = (0.8 + 0.065 \times U_{wind}) \times 10^{-3}$ where U_{wind} is wind speed) which gives slightly larger drag coefficient, C_D. For an unsteady flow, JELESNIANSKI *et al.* (1992) noted that weak turbulent mixing associated with low wind did not allow sufficient time to mix down to the bottom. Because of this transitional effect, they used higher $C_D (= 3 \times 10^{-3})$. HEAPS (1983) also pointed out that the wind drag coefficient depends on the state of development of the sea surface waves thus many surge models use higher C_D values than those suggested by air-sea interaction studies such as WU (1982).

The calculated u_{*_b} values were nearly identical in magnitude from both models (Figure 5). The directions of the bottom stress also were comparable for the high winds. The agreements between the models and the estimation from the log-fit of the observation data were reasonably good during the high wind period. Especially during the 3-day period between 10/10/94 and 10/13/94 with constant strong northerly winds, the model calculated value of u_{*_b} was in good agreement with the observation. All the peaks of bottom friction velocity in the order of 1 cm/sec were associated with strong

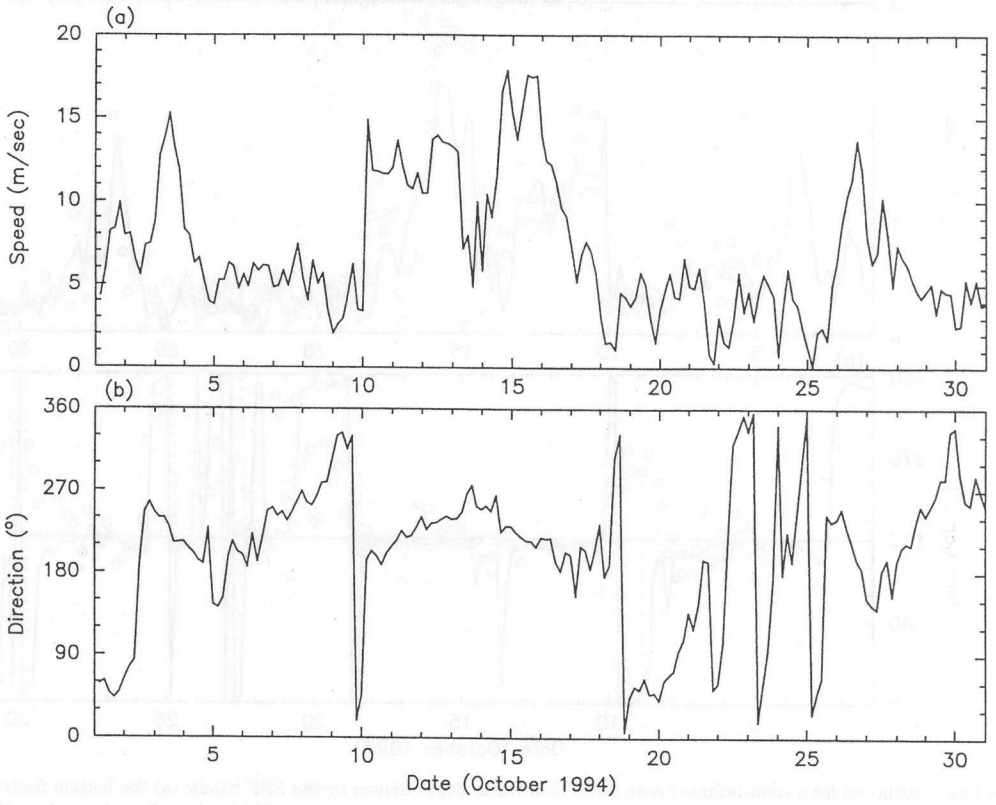

Figure 4. Surface winds during October 1994 recorded at the FRF pier; (a) the magnitude and (b) the direction clockwise from north (0° is alongshore toward north, 90° is offshore, 180° is alongshore toward south, and 270° is onshore directed, respectively). Horizontal axis represents the day in October 1994.

alongshore (~ 180°) and small offshore (< 180°) components which appear to be related to downwelling wind-driven currents. The abrupt shift in the flow direction coincide with rapid wind speed changes, which shows that the steady flow assumption cannot hold especially for the rapidly decelerating winds.

Around the storm peak for 10/16/94, the modeled bottom friction is still dominantly alongshore with weakly offshore component whereas the observation shows weakly onshore variation. Considering the error of up to 5° in the electromagnetic current sensors, we cannot be sure about the discrepancy between the modeled and observed directions. The underestimation of the modeled value of u_{*b} is also apparent during this period. With increased winds, also wave activity becomes dominant. GRANT and MADSEN (1986) demonstrated the increased u_{*b} and z_0 by the wave-current interaction. In the JM model, the constant bottom roughness, $z_0 = 2 \times 10^{-5}$ m based on $z_{0b}/h = 10^{-6}$ with $h = 20$ m, certainly is an underestimation for a condition of high waves. For the SLOSH model, the slip coefficient, s = 0.0009 m/sec, may be also increased under this situation. MASTENBROCK (1992) showed the role of the waves on the storm surges. There were counter-interactive effects of the wave ages by enhancing the effective sea surface roughness and the radiation stress of slow-down of the surge buildup. The swell in shallow water also enhanced the bottom friction, which may be the case around 10/16/94.

SUMMARY AND CONCLUSIONS

The SLOSH model, based on constant eddy viscosity and slip coefficient, reproduced reasonable steady bottom flow behavior of the wind-driven currents over an inner shelf. Comparison of the SLOSH model's asymptotic behavior to the JM model with more realistic bilinear eddy viscosity showed that the SLOSH model predicted the same behavior for shallow water (high u_{*s}/fh). The depth limitation was more relaxed for the depth averaged flow, which implies the successful storm surge prediction by the SLOSH model.

For the simple linear coastline such as in the MAB off North Carolina, the steady flow solution for the semi-infinite ocean was adequate to estimate the bottom stress from the wind-driven flow of extratropical origin. The inability of handling rapidly decelerating winds resulted in unrealistic direction variations. The additional wave effect by increasing surface and bottom roughness should be resolved by incorporating bottom boundary layer dynamics.

The bottom stress calculation showed the dominant along-

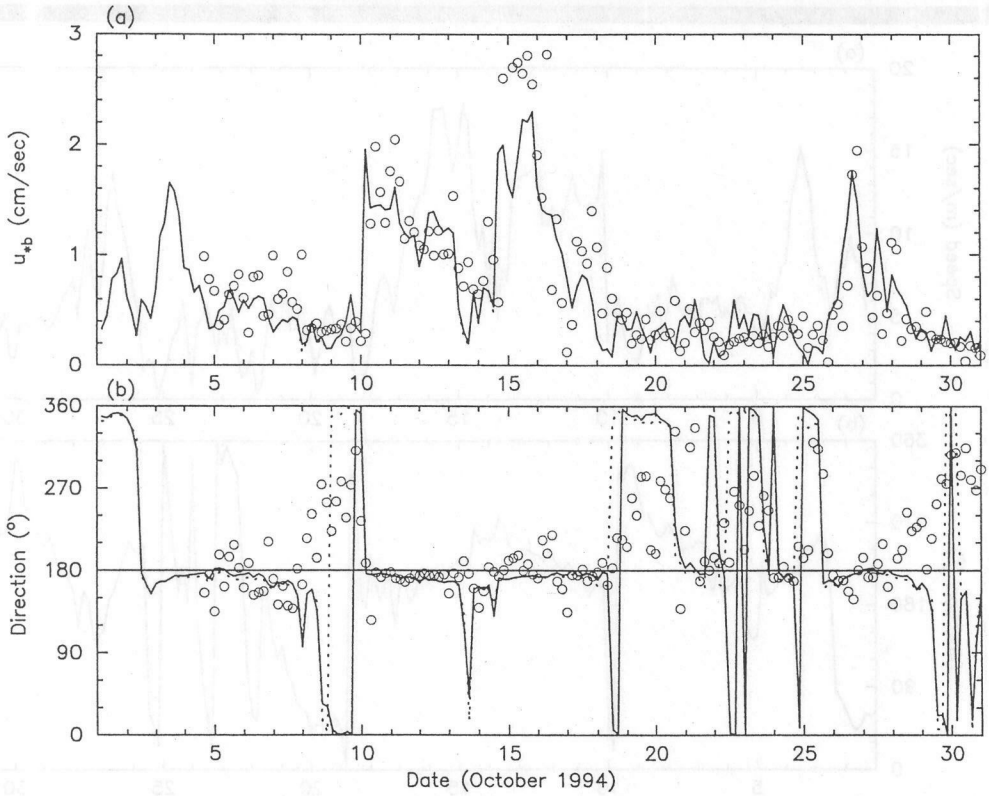

Figure 5. Steady flow simulation for a semi-infinite ocean with 20 m water depth driven by the FRF winds; (a) the bottom friction velocity, u_{*b}, and (b) the bottom flow direction clockwise from north (0° is alongshore toward north, 90° is offshore, 180° is alongshore toward south, and 270° is onshore directed, respectively). Horizontal axis represents the day in October 1994. Solid line represents the SLOSH model while the dotted line represents the JM model. One should note that both models give nearly identical u_{*b}. The open circle denotes the estimation from the VIMS deployment.

shore movement of the near-bottom flow. Under consistent northerly winds typical of extratropical meteorological conditions in the MAB, the secondary offshore components existed. The complications of the cross-shore transport direction of the near-bottom flow were caused by the approaching system with increasingly onshore-directed winds.

ACKNOWLEDGEMENTS

The partial support of this study came from the National Science Foundation as a component of the Coastal Ocean Processes (CoOP) study, Grant OCE-9123513. Dr. L.D. Wright is the PI of the VIMS component. The authors are grateful to the late Dr. Chester P. Jelesnianski who led the SLOSH model development. The authors are thankful for the encouragement from Dr. W.A. Shaffer, Chief, Marine Techniques Branch, Techniques Development Laboratory (TDL), National Weather Service (NWS), National Oceanic and Atmospheric Administration (NOAA). Discussions with Dr. J.M. Brubaker of VIMS were of great help in developing this manuscript. Mr. G.M. Sisson of VIMS is acknowledged for the editorial comments. This is Contribution Number 2136 from the Virginia Institute of Marine Science.

LITERATURE CITED

BLIER, W.; KEEFE, S.; SHAFFER, W.A., and KIM, S.-C., 1997. Storm surges in the region of western Alaska. *Monthly Weather Review,* 3094–3108.

DAVIES, A.M., 1988. On formulating two-dimensional vertically integrated hydrodynamic numerical models with an enhanced representation of bed stress. *Journal of Geophysical Research,* 95, 1241–1263.

GRANT, W.D. and MADSEN, O.S., 1986. The continental shelf bottom boundary layer. *Annual Review of Fluid Mechanics,* 18, 265–305.

HEAPS, N.S., 1983. Storm surges, 1967–1982. *Geophysical Journal of Royal Astronomical Society,* 74, 331–371.

JELESNIANSKI, C.P., 1970. Bottom stress time-history in linearized equations of motion for storm surges. *Monthly Weather Review,* 98, 462–478.

JELESNIANSKI, C.P.; CHEN, J., and SHAFFER, W.A., 1992. *SLOSH: sea lake, and overland surges from hurricanes.* NOAA Technical Report NWS 48, Department of Commerce, USA, 71 p.

JENTER, H.L. and MADSEN, O.S., 1989. Bottom stress in wind-driven depth averaged coastal flows. *Journal of Physical Oceanography,* 19, 962–974.

KIM, S.-C.; CHEN, J., and SHAFFER, W.A., 1996. An operational forecast model for extratropical storm surges along the US east Coast, *Proceedings, Conference on Oceanic and Atmospheric Prediction,* American Meteorological Society, 281–286.

KIM, S.-C.; WRIGHT, L.D., and KIM, B.-O., 1997. The combined ef-

fects of synoptic and local-scale meteorological events on bed stress and sediment transport on the inner shelf of the Middle Atlantic Bight. *Continental Shelf Research,* 17, 407–433.

KIM, S.-C.; CHEN, J.; PARK, K., and CHOI, J.K., 1998. Coastal surges from extratropical storms on the west coast of the Korean Peninsula. *Journal of Coastal Research,* in press.

LENTZ, S.J., 1994. Current dynamics over the northern California inner shelf. *Journal of Physical Oceanography,* 24, 2461–2478.

LENTZ, S.J., 1995. Sensitivity of the inner-shelf circulation to the form of the eddy viscosity profile, *Journal of Physical Oceanography,* 25, 19–28.

LENTZ, S.J. and C.D. WINANT, 1986. Subinertial currents on the southern California shelf. *Journal of Physical Oceanography,* 16, 1737–1750.

MASTENBROCK, C., 1992. The effect of waves on surges in the North Sea. *Coastal Engineering 1992,* 874–882.

PLATZMAN, G.W., 1963. *The dynamical prediction of wind tides on Lake Erie.* Meteorological Monographs 4, American Meteorological Society, 44 p.

WELANDER, P., 1961. Numerical prediction of storm surges. *Advances in Geophysics,* 8, 315–379.

WRIGHT, L.D., 1995. *Morphodynamics of inner continental shelves.* CRC Press, 241 p.

WU, J., 1982. Wind-stress coefficients over sea surface from breeze to hurricane. *Journal of Geophysical Research,* 87, 9704–9706.